OPEN ACCESS

Saudi Journal of Engineering and Technology
Abbreviated Key Title: Saudi J Eng Technol
ISSN 2415-6272 (Print) | ISSN 2415-6264 (Online)
Scholars Middle East Publishers, Dubai, United Arab Emirates
Journal homepage: https://saudijournals.com

Original Research Article

Heat Transfer Modelling of Multilayer Coated Tools During Turning of H13 Hardened Steel: Analogous Coating Layer Approach

Ipilakyaa T. D.[1*], Tuleun L. T.[1], Injor O. M.[1]

[1]Department of Mechanical Engineering, Joseph Sarwuan Tarka University, Makurdi, Nigeria

DOI: 10.36348/sjet.2024.v09i04.002 | **Received:** 06.03.2024 | **Accepted:** 15.04.2024 | **Published:** 17.04.2024

***Corresponding author:** Ipilakyaa T. D
Department of Mechanical Engineering, Joseph Sarwuan Tarka University, Makurdi, Nigeria

Abstract

This paper investigates the heat transfer of multi-layer coated tools. An analogous coating layer technique is used to compare multi-layered coated tools to mono-layer coating tools and develop a heat transfer model for mono-layered coating tools. The equivalent heat capacity, density, and thermal conductivity of the coating are determined based on the geometric size, initial conditions, and boundary conditions, given the tool rake face temperature. The heat transfer efficiency of the multilayer coating is significantly influenced by the coating layers, the thickness of the layer, and the coating material. The results show that the equivalent coating layer approach is suitable for calculating coating temperature enhancement in the cutting heat transfer. The calculation of cutting temperatures for multilayer-coated tools was conducted and subsequently compared to experimental findings, revealing an error margin of around 10%. The findings of this study indicate that analytical models are also suitable for modelling cutting temperatures in multi- layer coating designs.

Keywords: Heat Transfer, Cutting Temperature, Multi-Layer Coated Tool, Rake Face Temperature, Composite Coating, Equivalent Coating Layer, Thermal Diffusivity, Thermal Conductivity, Equivalent Volumetric Heat Capacity.

INTRODUCTION

Coated tools are increasingly used in cutting tools due to their ability to extend tool life, lower cutting temperatures, and enhance workpiece surface integrity. The use of advanced cemented carbides with various thin coating film architectures has significantly influenced the development of cutting tool materials. Most cutting tools are coated with thin layers of aluminum oxide (Al_2O_3), titanium carbide (TiC), titanium carbonitride (TiCN), and titanium nitride (TiN). These coatings increase tool life and cutting speed, making them more efficient in machining [1, 2].

The mechanisms of cutting heat generation, heat partition, and heat transport in coated tools have been extensively studied, as temperature is a crucial aspect of machining. The substrate and coating materials used on coated tools greatly influence these processes, particularly on multi-layer coated tools with several coating layers [3, 4]. Tools with thin coatings that are coated differ from uncoated ones in terms of how heat is transferred, partitioned, and distributed during cutting. The mechanical, thermophysical, and physical properties of each thin layer of multi-layer coated tools vary, leading to varying distributions of temperature and heat transport in coated tools [5, 6].

In the cutting heat transfer process, the coating material is crucial. Al_2O_3, one of the coating materials, performs better as a heat barrier. Al_2O_3 with a thermal barrier is used as the intermediate layer in several common coating topologies, making it a suitable choice for the coating. The heat transmission during the cutting of coated tools was examined to demonstrate the impact of coating thickness and material [7, 8]. Sahoo and Datta [9] used a numerical model to investigate how the coating material affected the coating's temperature distribution, finding that the temperature fall trend of the Al_2O_3-coated tool was quicker than that of the TiC and TiN-coated tools. Mohammed and Basturk's study [10] examined and evaluated how the thickness of the Al_2O_3 coating affected both the tool body and tool-chip contact temperatures.

The coating element content has an impact on the cutting heat transmission. Zhang *et al.*, [11]

investigated the heat transmission performance of TiAlN coated tools through orthogonal cutting experiments and finite element simulation. They found that Ti0.41 Al0.59 N coated tools have the ability to lower tool temperature and cutting heat generation in comparison to Ti0.55 Al0.45 N coated tools. Wang *et al.*, [12] used pulsed photothermal reflection to study the thermal conductivity of coated tools and found that the coatings' thermal conductivity decreased as the number of layers increased.

A major problem facing researchers in relation to the cutting temperature discussion was the effects of coating properties on heat generation, heat partition, tool-chip interface temperature, tool-workpiece interface temperature, and heat transfer or flux in the coated tools, especially the multi-layer coated tools [13]. Multi-layer coated tools have several coatings of various materials and thicknesses, as well as interfaces between coating and surface and between coating and coating. Variations in the thickness of the coating layer as small as a few nanometers might result in changes in the cutting temperature [14].

This research uses an analogous coating layer technique to compare multi-layer coated tools to mono-layer coated tools and develop a heat transfer model for mono-layer coated tools. The equivalent coating layer method for figuring out how to raise the coating temperature in the cutting heat transfer of multi-layer coated tools was tested using finite element simulation results. The heat transfer model of mono-layer coated tools is then used to determine the cutting temperature of multi-layer coated tools.

HEAT TRANSFER MODEL OF COATED TOOLS

The cutting process uses three heat sources: tool-chip, tool-workpiece, and shear deformation. Coated tools produce most of their heat near the tool-chip interface, replacing the three heat sources on the cutting tool rake face with a constant equivalent temperature, Tw. The monolayer coating thickness ranges from 1 to 8 μm, with a substrate thickness significantly thicker than the coating thickness. Coated tool cutting heat transfer is solid heat transfer with a boundary transfer issue. The heat transfer model of mono-layer coated tools is created based on geometric size, initial conditions, and boundary conditions, given the tool rake face temperature. Figure 1 displays the cutting deformation zone's boundary conditions and the heat transfer model [15, 16].

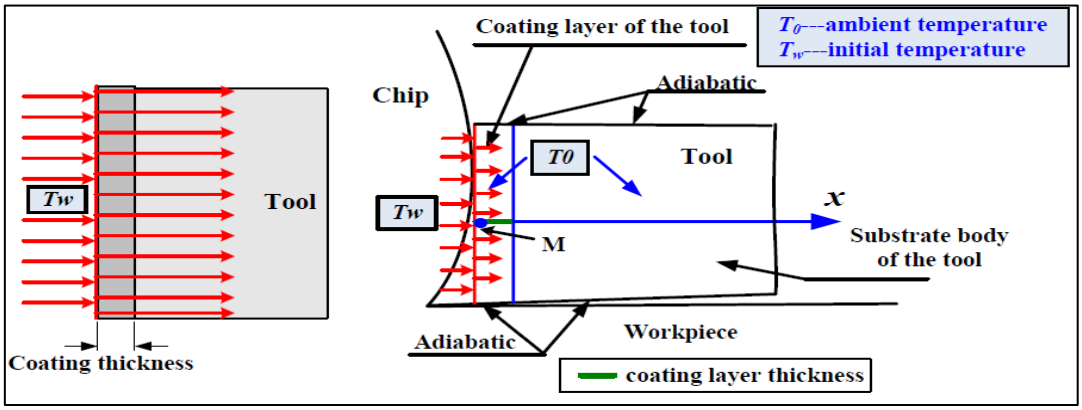

Figure 1: Schematic of coated tools heat transfer

The following assumptions are made in order to derive the model of the proposed heat transfer process: (1) thermal properties such as thermal conductivity and diffusivity are independent of temperature and they are uniform for coating layer; (2) in addition to the rake face, the rest of the surface is adiabatic surfaces; (3) tool coating and substrate $(x = d)$ has no additional heat resistance [17]. Through the above assumptions, the established heat transfer model of mono-layer coated tools is simplified to one-dimensional heat transfer model.

The cutting heat transfer model of mono-layer coated tools is derived from the Fourier heat transfer theory, neglecting the effect of heat transfer time. Rake face temperature and the other side of the substrate temperature are given. It is assumed that the heat transfer of the coating and substrate interface are normal, the temperature of coating and substrate are equal at the coating-substrate interface. Assuming that rake face temperature is T_w, environment temperature is T_0, initial temperature is $T_{initial} = T_0$, coating thickness is d, the thickness of the coated tools is L, and the cutting heat transfers is only along the thickness direction.

In the rectangular coordinate, the heat transfer differential equation is as follows:

$$\frac{\partial^2 T}{\partial x} = 0 \; 0 < x < L \qquad (1)$$

The initial conditions are:

$$\left.\begin{aligned} T|_{x=0} &= T_w \; 0 < x < d \\ T|_{x=L} &= T_0 \; d < x < L \end{aligned}\right\} \qquad (2)$$

Since the temperature and the heat flux at the coating and substrate interface are equal, it implies that:

$$\left.\begin{aligned} T_T|_{x=d} &= T_s|_{x=d} \\ -\lambda_c \frac{\partial T}{\partial x}\Big|_{x=d} &= -\lambda_s \frac{\partial T}{\partial x}\Big|_{x=d} \end{aligned}\right\} \quad (3)$$

Where T_T is the temperature of the tool coating, T_s is the temperature of the tool substrate, λ_c is the thermal conductivity of the tool coating and λ_s is the thermal conductivity of the tool substrate.

The general solution for equation (1) is:

$$T = c_1 x + c_2 \quad (4)$$

Solving the differential equations, we have:

$$\left.\begin{aligned} T(x) &= \frac{T_0 - T_w}{\frac{\lambda_s}{\lambda_c}(L-d)+d} x + T_w \; 0 < x < d \\ T(x) &= \frac{(T_0 - T_w)}{(L-d)+\frac{\lambda_s}{\lambda_c}d} x + \frac{(T_w - T_0)L}{(L-d)+\frac{\lambda_s}{\lambda_c}d} + T_0 \; 0 < x < d \end{aligned}\right\} \quad (5)$$

Equation (5) is referred to as the heat transfer model for mono-layer coated tools, where the coated tool temperature is related to the thermal conductivity of the coating, substrate and coating thickness. The temperature can be predicted when the parameters for the coated tool are known. According to equation (5), a decrease in the thermal conductivity of the coating leads to a reduction in the coating temperature.

Equivalent Coating Layer Method

The equivalent coating layer method has been recommended to simulate the interface temperature, cutting forces and some outputs of the cutting process for coated tools. The multi-layer coated tools can be equivalent to mono-layer coated tools using the equivalent coating layer approach. The equivalent thermal conductivity of the multi-layer coating may be determined using the 1-dimentional heat transfer principle of thermodynamics [18-20].

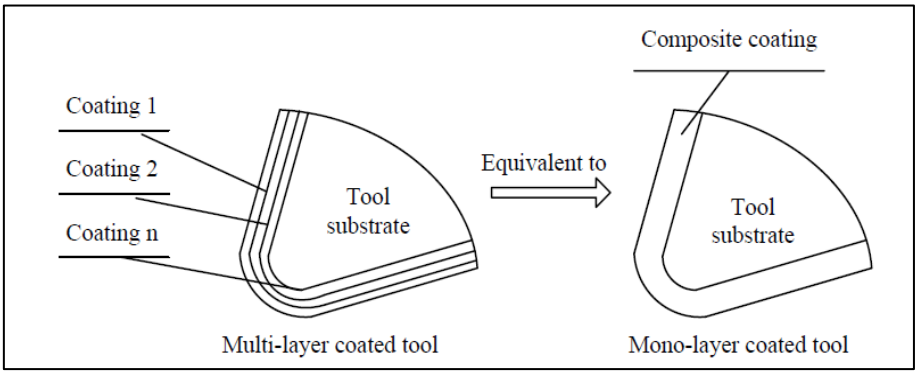

Figure 2: Equivalent modelling of Multi-layer coated tools

Figure 2 illustrates a multi-layer coating tool, which is illustrated as a mono-layer composite coating with 3-4 elements throughout its thickness. The equivalent thermal conductivity of the coating is significantly influenced by the coating layers, the thickness of the coating, and the coating material. The thermodynamics expression in equation (6) can be used to determine the properties of multi-layer coated tools [21, 22].

$$\frac{\sum_1^t x_i}{\lambda_{eq}} = \sum_1^t \frac{x_i}{\lambda_i} = \frac{x_1}{\lambda_1} + \frac{x_2}{\lambda_2} + \cdots \frac{x_t}{\lambda_t} \quad (6)$$

Where x_i is the thickness values of individual coating layers (i=1, 2, 3…n), λ_i is the thermal conductivities of individual coating layers (i=1, 2, 3…n), $\sum x_i$ is total thickness of the equivalent layer and λ_{eq} is the equivalent thermal conductivity of the equivalent layer.

The rake face temperature can be determined by quantifying the values of thermal diffusivity, expressed as $\frac{\lambda_{eq}}{C_{eq}}$, where C_{eq} is the equivalent volumetric heat capacity. The appropriate equation can be obtained by adding up the volumes of the separate layers V_i, to obtain the equivalent volume, V_{eq} of the coated tools. For an i-layer coating, the equivalent volume can be written as:

$$V_{eq} = V_1 + V_2 + V_3 + \cdots V_i \quad (7)$$

Where V_{eq} is the equivalent volume of the multi-layer coated tool, V_i is the volume of i-layers coating (i =1, 2, 3…t).

let ρ_i be the density of i-layers of multi-coated coated tools. By taking into account the adequate thicknesses, x_i and densities, ρ_i of each coating layers and substituting the density with $\rho_i = \frac{C_i}{c_{pi}}$, where, C_i is heat capacity of the i-layer and c_{pi} is the specific heat of the i-layer. The proposed model can now be written as:

$$\frac{\sum_i^t (x_i \rho_i c_{pi})}{C_{eq}} = \frac{x_1 \rho_1 c_{p1}}{C_1} + \frac{x_2 \rho_2 c_{p2}}{C_2} + \cdots \frac{x_i \rho_i c_{pi}}{C_i} \quad (8)$$

From equation (8), the multi-layer coated tools is considered equivalent to mono-layer coated tools. From (6) and (8), the thermal conductivity and thermal diffusivity of equivalent mono-layer composite coating can be obtained.

Simulation of Multi-Layer Coated Tools Using Finite Element Analysis

The orthogonal metal cutting simulation employs finite element simulation method which is dependent on the Lagrange techniques and explicit dynamic, thermo-mechanically coupled model software with adaptive refinement. The coated tool geometry and cutting parameters are as shown in Table 1.

Table 1: Coated tools geometry and cutting parameters

	TiAlN/TiN	TiN/TiC/TiN
Corner radius (mm)	0.02	0.02
Rake angle (°)	5.0	5.0
Flank angle (°)	5.0	5.0
Cutting speed (m/min)	40,60,90,120,200,250	40,60,90,120,200,250
Feed speed (mm/r)	0.2	0.2
Cutting depth (mm)	0.25	0.25
Cutting length (mm)	3.0	3.0

As shown in Figure 3, a finite element simulation model is created based on the geometry of multi-layer coated tools and cutting circumstances. The workpiece is made rectangular with dimensions of 3mm by 0.7mm. The grid number for the multi-layer coated tools was set to 100,000 using local grid refinement technology. The tooltip has been improved with a minimum side length of the grid as 0.1 mm. For the refining of the tool and workpiece contact area, the minimum side length of the grid is set at 0.2 mm.

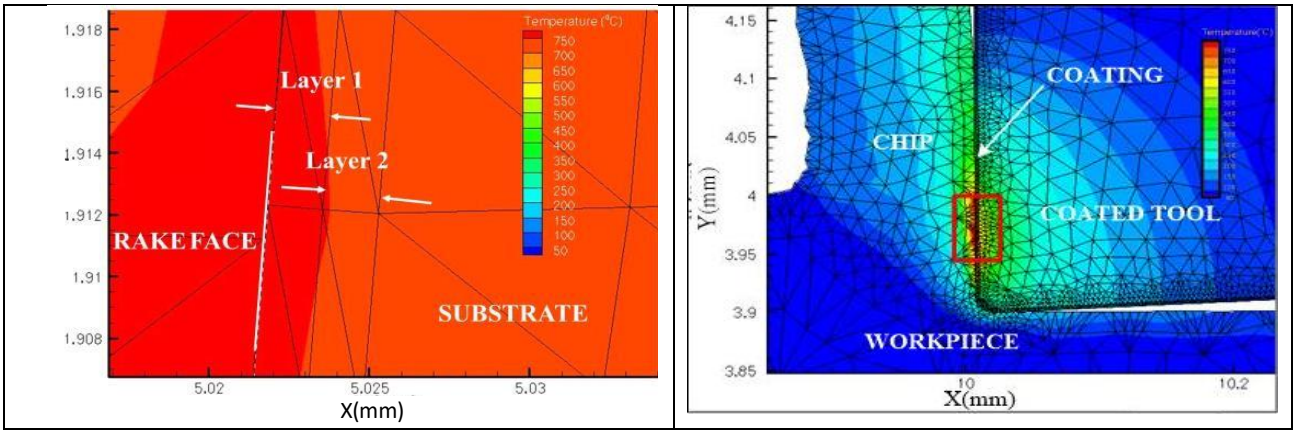

A **B**

Figure 3: Schematic diagram of the cutting temperature distribution (a) coated tool and (b) TiAlN/TiN coating

Experimental Setup

Temperature measurements were conducted in an experiment employing a thermocouple sensor on a cylindrical rod that is 300 mm long and has an exterior diameter of 70 mm. An experiment involving cutting was conducted using a CNC lathe machine (T6-series). The material utilized for the turning experiment is H13 hardened steel. Table 2 provides the chemical composition of H13 hardened steel, while Table 3 presents its physical and mechanical properties of the hardened steel. The cutting tools are coated with many layers, specifically TiAlN/TiN and TiN/TiC/TiN.

Table 2: Chemical composition of experimental materials H13 hardened steel [w/%]

Chemical component	C	Si	Mn	Cr	Mo	V	P	S
GB/T1299-2000	0.32~ 0.45	0.80~ 1.20	0.20~ 0.50	4.75~ 5.50	1.10~ 1.75	0.80~ 1.20	≤0.03	≤0.03

Figure 4 shows the thermocouple integrated into the turning tool. The tool with a protective coating was used to drill two holes for inserting the thermocouple sensor. The holes were sealed with a thin epoxy to avoid potential damage caused by cutting chips. The signals were transmitted from the sensor to the computer via the amplifier and A/D converter.

Table 3: Physical and mechanical properties of experimental materials H13 hardened steel

Properties	H13
Density ρ （kg/m^3）	7800
Thermal conductivity λ（W/m℃）	28.6
Young's modulus E（GPa）	211
Yield stress σ_s(MPa)	1075.6
Hardness（HRC）	48~52
Heat capacity C（J/kg℃）	460
Thermal diffusivity a（m^2/s）	7.92×10^{-6}

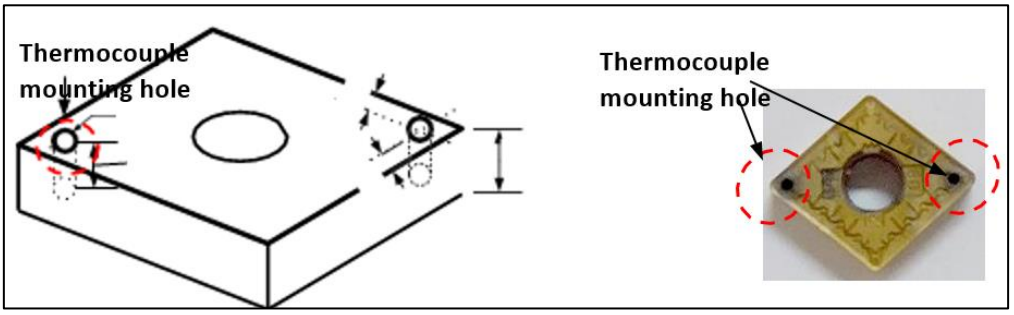

Figure 4: (a) schematic and (b) actual photograph of the tool sample with thermocouple mounting hole

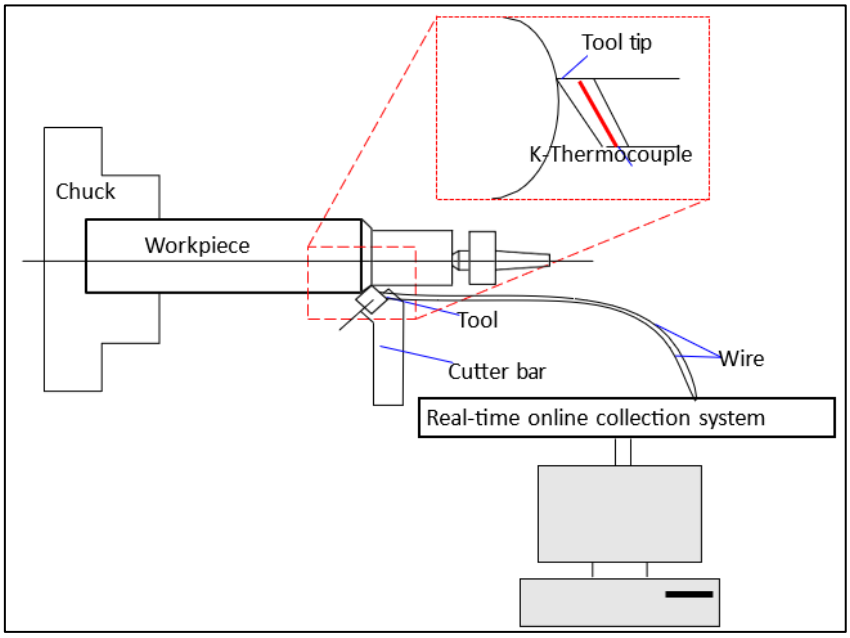

Figure 5: Setup for measuring tool temperature

Figure 5 displays a summary of the experimental setup. The feed rate set was f=0.2 mm/rev while the depth of cut was set at a_p=0.2 mm. The machining process was carried out with a consistent chip size and a consistent cutting velocity. The data collected by thermocouple sensors was recorded using a computer.

RESULTS AND DISCUSSIONS

The Equivalent Parameters of Multi-Layer Coated Tools

Figure 6 is the image of the scanning electron microscopy (SEM) of the tools coated with TiAlN/TiN and TiN/TiC/TiN multi-layers. Table 4 shows the mechanical and thermal characteristics of each layer in the multi-layer coated tools [6, 11, 20, 23-28]. From Table 2, the thermal conductivity of the multi-layer coated tools was determined at 500℃ using the thermal conductivity and thickness of each layer. The volumetric heat capacity of the multi-layer coated tools is 3.34 and 2.91 J/m^3 ℃, respectively. The equivalent thermal diffusivity is calculated using the determined values of equivalent heat capacity, density, and thermal conductivity of the multi-layer coated tools.

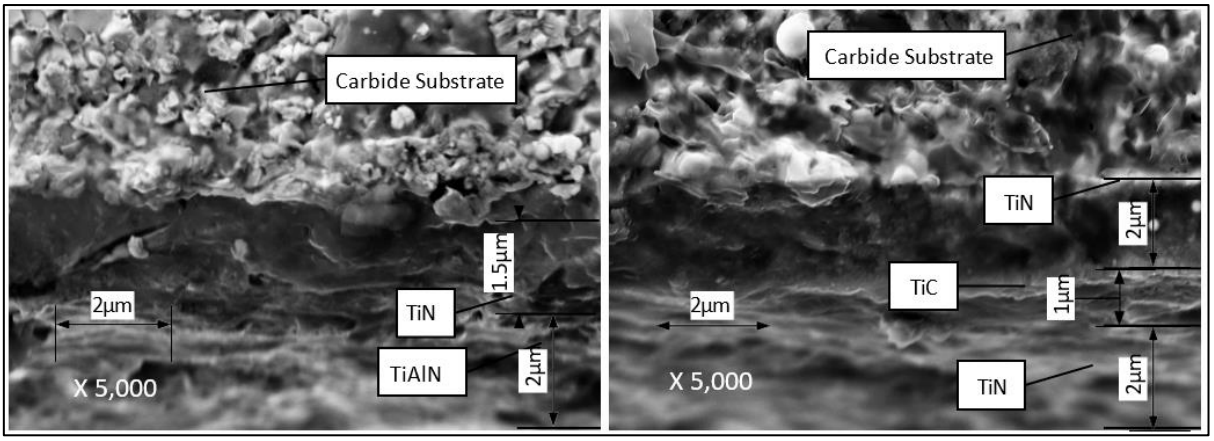

(a) TiAlN/TiN (b) TiN/TiC/TiN

Figure 6: SEM structure of carbide substrate and components of TiAlN/TiN and TiN/TiC/TiN. Magnification: .5000×

Table 4: Mechanical and thermal properties of multi-layer coated tools

Coating	TiC	TiN	TiAlN	TiAlN/TiN	TiN/TiC/TiN
Young's modulus E(GPa)	450-496	250	370		
Density ρ(kg/m^3)	4650-4900	4650	1892		
Thermal conductivity(500°C) λ(W/m °C)	37	23	15.4	15.1	24.25
Heat capacity C_{eq} (J/m^3°C)	2.55	3	3.6	3.34	2.91

The mono-layer composite coating for TiAlN/TiN has an equivalent thickness of 3.5µm, whereas the TiN/TiC/TiN multi-layer coated tools have an equivalent thickness of 5µm.

Heat Transfer Modeling from Calculated Results

The cutting temperature for the mono-layer composite coating can be estimated using Equation (5). Figure 7 represents the temperature analysis where increasing the coating thickness decreases the cutting temperature of the coating. The absence of a temperature differential at the coating interface is a result of the multi-layer coating being equivalent to a mono-layer composite coating. The cutting temperature at the first coating layer of the TiAlN/TiN coated tool is less compared to that of the TiN/TiC/TiN coated tool. The heat transfer efficiency of the TiN/TiC/TiN coating is superior to that of TiAlN/TiN coated tool. A TiN/TiC/TiN multi-layer coated tool with a coating thickness of 5µm is more effective in reducing cutting temperature than a TiAlN/TiN multi-layer coated tool with a coating thickness of 3.5µm.

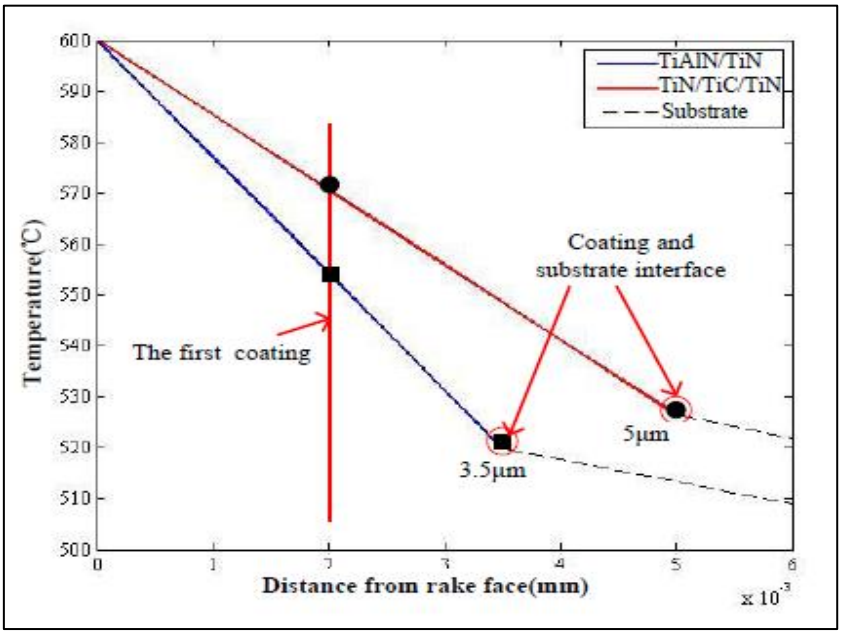

Figure 7: Cutting temperature of the equivalent mono-layer composite coating for TiAlN/TiN and TiN/TiC/TiN multi-layer coated tools

The temperature of cut of the multi-layer coated tools depends on various factors, including the thermal physical properties of the coating material and substrate material, the friction coefficient between the coating and workpiece, and the distribution of cutting heat between the cutting tool and coating structure. The heat transfer performance of multi-layer coated cutting tools is influenced by the thermal physical properties of the coatings, especially when the coatings have the same structure and thickness. By employing the equivalent coating layer method, a multi-layer coating is considered equivalent to a mono-layer composite coating.

Finite element simulation of tools with multi-layer coatings and tools with mono-layer composite coatings

Figure 8 shows the results of the Finite Element simulation. The results for temperature include rake face temperature, coating and substrate interface temperature for multi-layer coated tools (TiAlN/TiN and TiN/TiC/TiN) and equivalent mono-layer composite coated tools. The average temperature is the result of the temperature of the rake face and the coating-substrate temperature.

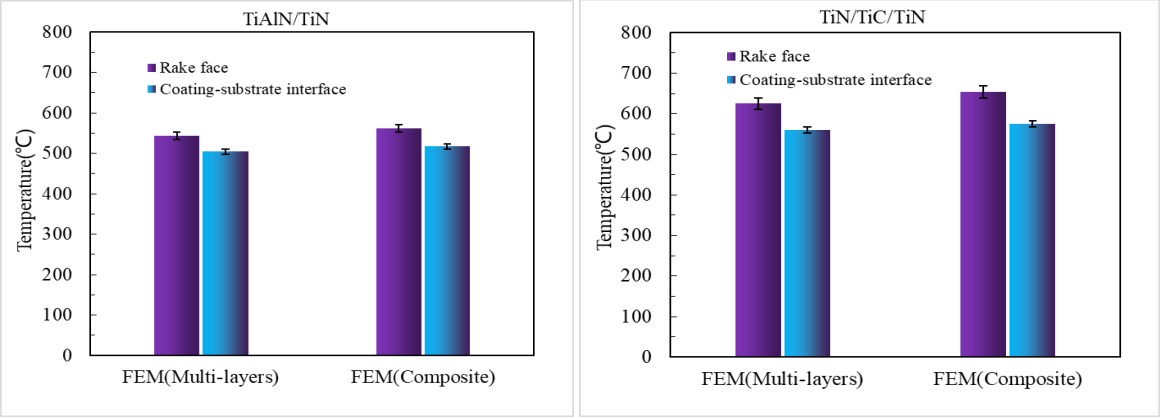

Figure 8: The finite element simulation results of multi-layer coatings and mono-layer composite coatings at a cutting speed of *v*=120m/min

From the analysis above, the inaccuracy in rake face temperature simulation modeling is 3.3% for the TiAlN/TiN coated tool and 4.6% for the TiN/TiC/TiN coated tool. The inaccuracy in the interface temperature simulation modeling is 2.6% for the TiAlN/TiN coated tool and 2.5% for the TiN/TiC/TiN coated tool. The discrepancies in simulated temperatures are minimal.

Experimental Results

The experimental evaluations of the cutting temperature of TiAlN/TiN and TiN/TiC/TiN multi-layer coating tools are depicted in Figure 9. The temperature at the measurement spot exhibited a progressive increase when the cutting speed was increased.

At a cutting speed of 120 m/min, the internal measuring point temperature of TiAlN/TiN and TiN/TiC/TiN multi-layer coated tools was found to be 426℃ and 494℃, respectively. In Figure 10, the temperature values for the TiAlN/TiN and TiN/TiC/TiN multi-layer coating tools were calculated and experimentally measured. The temperatures of the rake face were estimated using a rake face temperature model [11]. The temperatures of the coating-substrate interface were determined using heat transfer modeling. The temperature measurements at the measuring site (2.5 mm from the rake face) were obtained through experimentation. The experimental temperature was compared to the calculated temperature, revealing an inaccuracy of 9.8% for the TiAlN/TiN multi-layer coating tool and 5.4% for the TiN/TiC/TiN multi-layer coating tool.

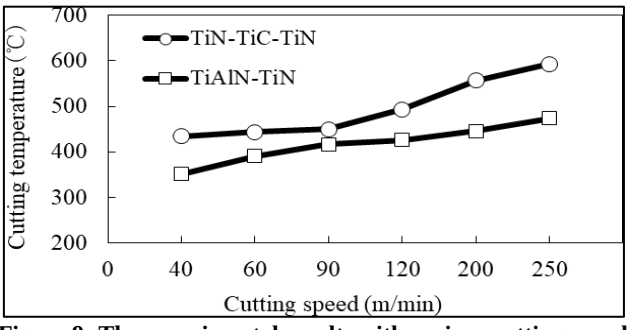

Figure 9: The experimental results with various cutting speed

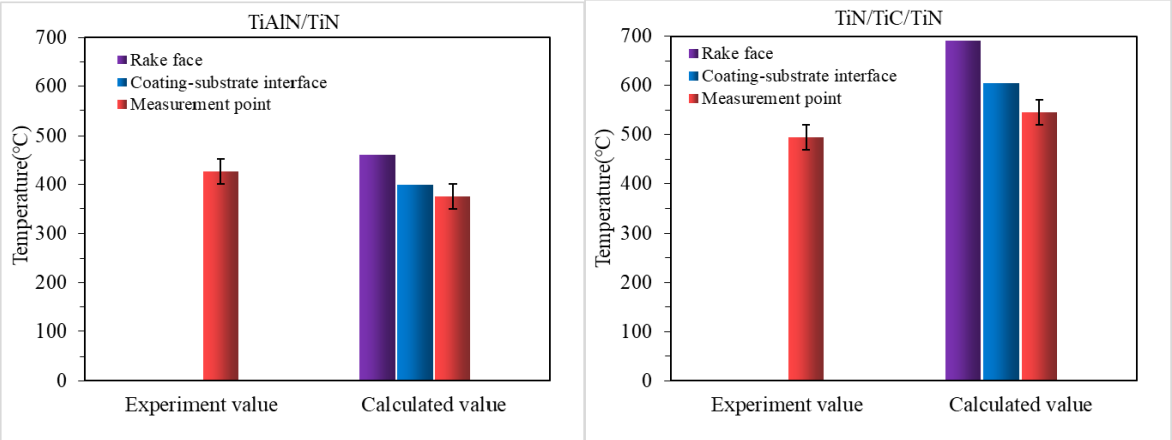

Figure 10: Experimental and calculated results of TiAlN/TiN and TiN/TiC/TiN multi-layer coated tools at v=120m/min

CONCLUSION

This paper investigates the cutting temperature of multi-layer coated tools. The cutting temperatures of multi-layer coated tools can be determined using analytical models.

The primary findings can be summarized as follows:

The agreement between the equivalent coating layer model for multi-layer coating and the multi-layer coating model in FEM predictions is in good agreement, with a difference of less than 5%.

The findings of this study indicate that analytical models are also suitable for modelling cutting temperatures in multi-layer coating designs. The calculation of cutting temperatures for multi-layer coated tools was conducted and subsequently compared to experimental findings, revealing an error margin of around 10%.

The prediction of rake face temperatures and coating-substrate interface temperatures is crucial in practical applications. These temperatures can assist in selecting appropriate coated tools for specific machining parameters, thereby preventing excessive thermal loading on the tools. Additionally, they enable the rational selection of coated tools to enhance machining performance and extend tool lifespan.

REFERENCES

1. Rizzo, A., Goel, S., Luisa Grilli, M., Iglesias, R., Jaworska, L., Lapkovskis, V., Novak, P., Postolnyi, B.O., & Valerini, D. (2020). The critical raw materials in cutting tools for machining applications: A review. *Materials*, 13(6), 1377.
2. Sousa, V. F. C. & Silva, F. J. G. (2020). Recent advances in turning processes using coated tools—A comprehensive review. *Metals*, 10(2), 170.
3. Du, J., Hao, T., Zhang, X., Su, G., Zhang, P., Sun, Y., Zhang J. & Xu, C. (2021). Finite element investigation of cutting performance of Cr/W-DLC/DLC composite coated cutting tool. *The International Journal of Advanced Manufacturing Technology*, 118, 2177–2192.
4. Zhao, J., Liu, Z., Ren, X., Wang, B., Cai, Y., Song, Q., & Wan, Y. (2022). Coating-thickness-dependent physical properties and cutting temperature for cutting Inconel 718 with TiAlN coated tools. Journal of Advanced Research, 38, 191-199.
5. Dabees, S., Mirzaei, S., Kaspar, P., Holcman, V., & Sobola, D. (2022). Characterization and evaluation of engineered coating techniques for different cutting tools. *Materials*, 15(16), 5633.
6. Zhang, J., Zhang, G., & Fan, G. (2022). Effects of tool coating materials and coating thickness on cutting temperature distribution with coated tools. *International Journal of Applied Ceramic Technology*, 19(4), 2276-2284.
7. Zhang, Z., Zeng, W., Zhang, X., & Zeng, Y. (2024). Comparative Study on Different Methods for Prediction of Thermal Insulation Performance of Thermal Barrier Coating Used on Turbine Blades. *Journal of Thermal Science.* 33, 172–189.
8. Qiu, S., Liu, Y. C., Guo, H., Huang, C. G., Ma, Y., & Wu, C. W. (2020). Effect of splat-interface discontinuity on effective thermal conductivity of plasma sprayed thermal barrier coating. *Ceramics International*, 46(6), 4824-4831.
9. Sahoo, S. P., & Datta, S. (2022). Comparative experimental study on application feasibiility of MTCVD TiCN-Al 2 O 3-TiOCN multi-layer coated carbide and PVD TiN single layer coated composite ceramic inserts during dry machining of Ti-6Al-4V. *Sādhanā: Academy Proceedings in Engineering Sciences*, 47(105), 1-25.
10. Mohammed, K., & Baştürk, S. (2022). Numerical study of heat transfer aspects in cutting tools made of Al2O3, ZrB2, TiB2, TiN using ANSYS fluent software. *Niğde Ömer Halisdemir Üniversitesi Mühendislik Bilimleri Dergisi*, 11(1), 222-231.
11. Zhang, J., Liu, Z., Xu, C., Du, J., Su, G., Zhang, P., & Meng, X. (2021). Modeling and prediction of cutting temperature in the machining of H13 hard steel of multi-layer coated cutting tools. *The*

International Journal of Advanced Manufacturing Technology, 115(11), 3731-3739.

12. Wang, H., Huang, B., Dong, J., Chung, J. N., & Hartwig, J. W. (2024). Enhancement and optimization of cryogenic metal tube chilldown heat transfer using thin-film coating, I. Effects of flow mass flux and coating layer thickness. *International Communications in Heat and Mass Transfer*, 153, 107368.
13. Hao, G. & Liu, Z. (2020). Thermal contact resistance enhancement with aluminum oxide layer generated on TiAlN-coated tool and its effect on cutting performance for H13 hardened steel. *Surface and Coatings Technology*, 385, 125436.
14. Vereschaka, A., Tabakov, V., Grigoriev, S., Sitnikov, N., Milovich, F., Andreev, N., Sotova C., & Kutina, N. (2020). Investigation of the influence of the thickness of nanolayers in wear-resistant layers of Ti-TiN-(Ti, Cr, Al) N coating on destruction in the cutting and wear of carbide cutting tools. *Surface and Coatings Technology*, 385, 125402.
15. Hao, G., & Liu, Z. (2020). The heat partition into cutting tool at tool-chip contact interface during cutting process: a review. *The International Journal of Advanced Manufacturing Technology*, 108, 393-411.
16. Mane, S., Joshi, S. S., Karagadde, S., & Kapoor, S. G. (2020). Modeling of variable friction and heat partition ratio at the chip-tool interface during orthogonal cutting of Ti-6Al-4V. *Journal of Manufacturing Processes*, 55, 254-267.
17. Yang, M., Li, C., Luo, L., Li, R., & Long, Y. (2021). Predictive model of convective heat transfer coefficient in bone micro-grinding using nanofluid aerosol cooling. *International Communications in Heat and Mass Transfer*, 125, 105317.
18. Grzesik, W. (2020). Modelling of heat generation and transfer in metal cutting: a short review. *Journal of Machine Engineering*, 20(1), 24–33.
19. Al-Tameemi, H. A., Al-Dulaimi, T., Awe, M. O., Sharma, S., Pimenov, D. Y., Koklu, U., & Giasin, K. (2021). Evaluation of cutting-tool coating on the surface roughness and hole dimensional tolerances during drilling of Al6061-T651 alloy. *Materials*, 14(7), 1783.
20. Bencheikh, I., Nouari, M., & Bilteryst, F. (2020). Multi-step simulation of multi-coated tool wear using the coupled approach XFEM/multi-level-set. *Tribology International*., 146, 106034.
21. Yan, Y., Zhuang, Y., Ouyang, H., Hao, J., & Han, X. (2024). Experimental investigation on optimization of the performance of gallium-based liquid metal with high thermal conductivity as thermal interface material for efficient electronic cooling. *International Journal of Heat and Mass Transfer*, 226, 125455.
22. Younes, H., Mao, M., Murshed, S. S., Lou, D., Hong, H., & Peterson, G. P. (2022). Nanofluids: Key parameters to enhance thermal conductivity and its applications. *Applied Thermal Engineering*, 207, 118202.
23. Karaguzel, U. (2021). Transient multi-domain thermal modeling of interrupted cutting with coated tools. The International Journal of Advanced Manufacturing Technology, 116(1), 345-361.
24. Zha, X., Wang, T., Chen, F., Wang, J., Lin, L., Lin, F., ... & Jiang, F. (2022). Investigation the fatigue impact behavior and wear mechanisms of bilayer micro-structured and multilayer nano-structured coatings on cemented carbide tools in milling titanium alloy. *International Journal of Refractory Metals and Hard Materials*, 103, 105738.
25. Ranjan, P. & Hiremath, S. S. (2022). Finite element simulation and experimental validation of machining martensitic stainless steel using multi-layered coated carbide tools for industry-relevant outcomes. *Simulation Modelling Practice and Theory*, 114, 102411.
26. Moganapriya, C., Vigneshwaran, M., Abbas, G., Ragavendran, A., Ragavendra, V. H., & Rajasekar, R. (2021). Technical performance of nano-layered CNC cutting tool inserts–An extensive review. *Materials Today: Proceedings*, 45, 663-669.
27. Bhandarkar, L. R., Behera, M., Mohanty, P. P., & Sarangi, S. K. (2021). Experimental investigation and multi-objective optimization of process parameters during machining of AISI 52100 using high performance coated tools. *Measurement*, *172*, 108842.
28. Ipilakyaa T.D., Bam S.A., & Tuleun L.T. (2023). Prediction of Cutting Temperature Distribution in Transient Heat Conduction of Monolayer Coated Tools Based on Non-Fourier Heat Conduction During Machining of H13 Hard Steel. *International Journal of Engineering Research & Science*, *9*(8), 1-10.